EVIDENCE FOR EXCESS PORE PRESSURES IN SOUTHWEST INDIAN OCEAN SEDIMENTS

Dallas Abbott[1], William Menke[1], Michael Hobart, and Roger Anderson[1]

Lamont-Doherty Geological Observatory of Columbia University, Palisades, New York 10964

Abstract. Brown clay cores from the Madagascar and Crozet basins show the following evidence of excess pore pressures: large amounts of flow-in, increasing average sedimentation rate with age, and nonlinear temperature gradients. Additionally, many hilltops in these basins have no visible sediment cover. The bare hilltops may result from periodic slumping caused by excess pore pressures. Calculated excess pore pressures which equal or exceed the overburden pressure were inferred from water fluxes predicted by nonlinear temperature gradients and laboratory permeability measurements by using Darcy's law. Since pore pressures which exceed the overburden pressure are unreasonable, we attribute this discrepancy to laboratory measurements which underestimate the in situ permeability. The widespread presence of overpressured sediments in areas of irregular topography provides a process for resuspension of clay-sized particles. This mechanism does not require high current velocities for the erosion of clay and therefore can be applied to many areas where no strong currents are evident. Carbonate-rich sediments from the Madagascar Ridge, the Mozambique Ridge, and the Agulhas Plateau had almost no flow-in and occurred in areas where all topography was thickly draped with sediment. Since the age and tectonic location of the ridges and plateaus preclude water circulation in the basement, we attribute these differences between the brown clay and the carbonate-rich material to an absence of significant excess pore pressures in the plateau and ridge sediments.

Introduction

Nonlinear temperature profiles have been observed at several locations in the oceans [Anderson et al., 1979]. There are a number of mechanisms which may cause such gradients: e.g., large thermal conductivity changes with depth, water movement through the sediments, bottom water temperature changes, and internal heat generation in the sediments. Although each of these mechanisms may be applied to certain examples, convection of water through the sediments best explains the heat flow pattern in young oceanic areas [Anderson et al., 1977]. The areas in the Indian Ocean where convection is probably the primary cause of nonlinear temperature profiles have the following characteristics: (1) the basement age is young, 55 m.y. or less, (2) sediment cover is thin, generally less than 150-250 m, and (3) the observed average apparent heat flow is much less than that predicted by theoretical conductive models of heat transfer [Parsons and Sclater, 1977]. (Because the theoretical models predict the increase in depth of the

oceanic crust away from oceanic ridges, we believe that these models adequately represent the total heat loss of the oceanic lithosphere.) When the heat transfer due to convection of water through the sediments is added to the conductive component, the average heat flow in these areas approaches the theoretical prediction. The fact that inclusion of convection in the top surface of an otherwise conductively cooling lithosphere allows heat flow and topography data to be consistent is itself a strong argument for a convective interpretation of the sediment temperature profiles.

The possible existence of water movement through the sediments covering the oceanic basement has important implications for the consolidation of the sediment. If the water movement is rapid enough and the permeability of the sediment is low enough, convection of water will be accompanied by noticeable excess pore pressures. We define excess pore pressure as the in situ water pressure in excess of the hydrostatic pressure. Excess pore pressures accompanied by low permeabilities slow down the consolidation of the sediment, thus decreasing the effective weight of the overburden. Such high pore pressures can be detected by direct measurement or by looking at the variation of sediment physical properties with depth. For the data we shall discuss, the progress of consolidation is inferred from observation of physical properties.

We measured three sedimentary parameters which change systematically with depth as a result of compaction: permeability, porosity, and thermal conductivity. The total change in porosity and thermal conductivity is only a few percent in our piston cores: scarcely higher than the error of measurement. In contrast, permeability often changes by an order of magnitude within 10 m, while the relative error remains at 5 to 25%. It is for this reason that we have chosen permeability profiles as a tool with which to observe consolidation.

Although permeability, water movement, and consolidation are interrelated, they do not correlate perfectly. Permeability is affected by grain size distribution as well as by the porosity of the sediment. Consolidation is affected not only by permeability and water movement but also by the sedimentation rate and the total sediment thickness. These factors must all be considered when using permeability versus depth profiles to study consolidation.

The cores used in this study are from the Southwest Indian Ocean (Figure 1). Two broad types of sediment exist in the cores: brown clays and calcareous sands and muds. The brown clays are from 18 to 55 m.y. old oceanic crust in the Crozet and Madagascar basins [Schlich, 1975]. The calcareous sands and muds are from the Agulhas Plateau, the Madagascar Ridge, and the Mozambique Ridge, all of which are at least 55 and probably in excess of 80 m.y. old [Saito et al., 1974; Simpson et al., 1972]. The environments of the two sediment types are quite different. The brown clays are all from areas where basement outcrops are visible and the

---

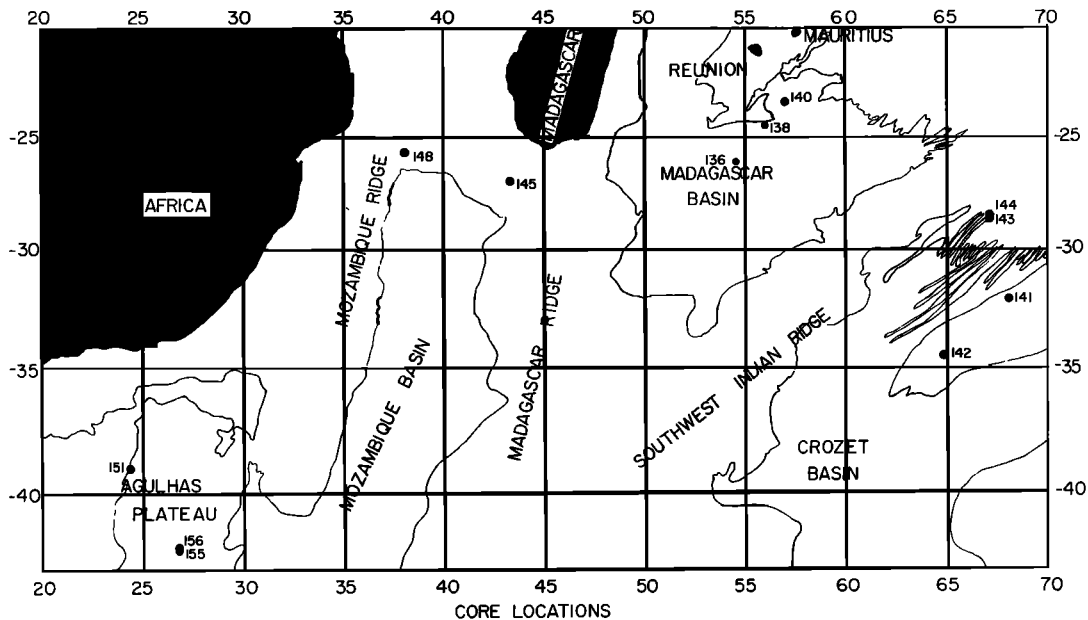[1] Also at the Department of Geological Sciences, Columbia University, New York 10027.

Fig. 1. Dots are locations of piston cores taken in the Southwest Indian Ocean during
Vema 3409, 3410, and 3411.

maximum sediment thickness is less than 250 m.
The calcareous sands and muds are located in places
where the sediment thickness greatly exceeds 250 m.
and outcropping acoustic reflectors are not basalt
basement [Tucholke and Carpenter, 1977]. The dif-
ference in the environment of the two sediment
types should result in different consolidation
histories.

Although sedimentation rates are slightly higher
in the calcareous sands and muds than in the brown
clays, the accumulation rate in both areas is much
lower than the 85/m/m.y. rate which Trabant [1977]
found to be the maximum sedimentation rate for nor-
mally consolidated sediments. That is, all sedi-
ments with sedimentation rates higher than 85 m/
m.y. were found to be underconsolidated due to ex-
cess pore pressures induced by impeded dewatering
of rapidly accumulating sediment [Trabant et al.,
1975; Keller and Bennett, 1973]. Therefore in
both regions, excess pore pressures caused by ra-
pid sedimentation are unlikely.

The difference in age and total sediment thick-
ness between the two groups of sediment results in
totally different expectations for water movement
caused by convection. The brown clays are from
areas where nonlinear temperature gradients are
most likely to be the result of water movement.
Water movement through the calcareous sands and
muds is unlikely to be rapid enough to affect tem-
perature profiles or consolidation in surface sedi-
ments seriously, since the total sediment thick-
nesses are too great and the crust is too old to
support an active convective system. Because of
these major differences we will initially examine
the brown clays and the calcareous sands and muds
separately.

Brown Clays

The cores from the Madagascar and Crozet basins
were taken as part of a program which included de-
tailed heat flow surveys of small areas [Anderson

et al, 1979]. Each of the four areas surveyed had
a slightly different character and heat flow pat-
tern.

Cores 144 and 143 are from an 18 m.y. age sur-
vey area in the Crozet Basin. This was the young-
est area surveyed, with about 10-20 m of sediment
draping the basement. The steeper hillsides and
some hilltops have no sediment cover at all (Fig-
ure 2 and Figure 3). The 3.5-kHz precision depth
recorder (PDR) records for cores 143 and 144 show
the irregular sediment cover particularly well
(Figure 3). The area just downslope of core 143
has a hump of sediment which may well be a slump
or slide block. Slumps and slides are character-
ized on 3.5-kHz PDR records by irregular hummocky
surfaces of low reflectance and lack of internal
layered reflections [Embley and Jacobi, 1977].
The sediment of low reflectance at the base of the
slope where core V34-144 was taken could also be
a slide mass. The top of the slope in the area of
core V34-143 and the slope to the right show sedi-
ment thicknesses of up to 55 m, even though the
hill is often steeper than at V34-143. Although
the lack of sediment on the sides of the hills
at V34-143 and V34-144 could be due to current
erosion, such erosion is generally most evident
at the bases of slopes rather than on hillsides.
We therefore believe that some other mechanism
than current erosion is causing the uneven sedi-
ment distribution in the vicinity of cores V34-
143 and V34-144.

In the 18 m.y. survey area, 13 temperature gra-
dients out of 20 were nonlinear. Even corrected
for convection, the heat flow does not reach the
theoretical; perhaps because the areas of open
rock act as chimneys. Core V34-143 was not accom-
panied by temperature gradient measurements but is
of interest because it cored the sediment-basement
interface (Figure 3). The uppermost third of the
core is completely pelagic, while the remaining
part of the core contained a large quantity of
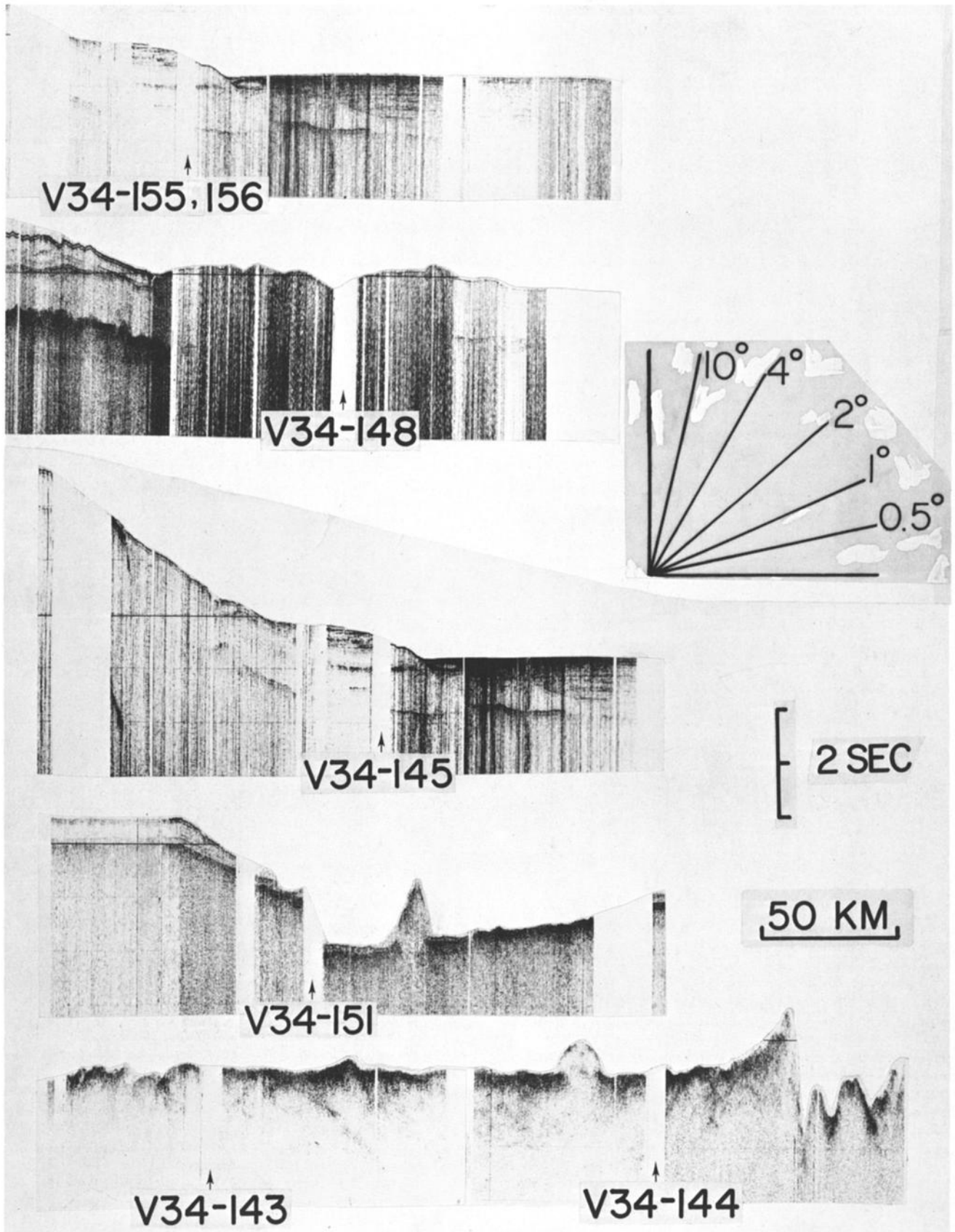rock fragments. The permeabilities of the two

Fig. 2. Profiler records of the sedimentary environment near cores 143, 144, 145, 148, 151, 155, and 156. One second of two-way travel time equals 400 fathoms (759 m). The slopes and distances are calculated for a speed averaging about 9 knots/h (16.65 km/h).
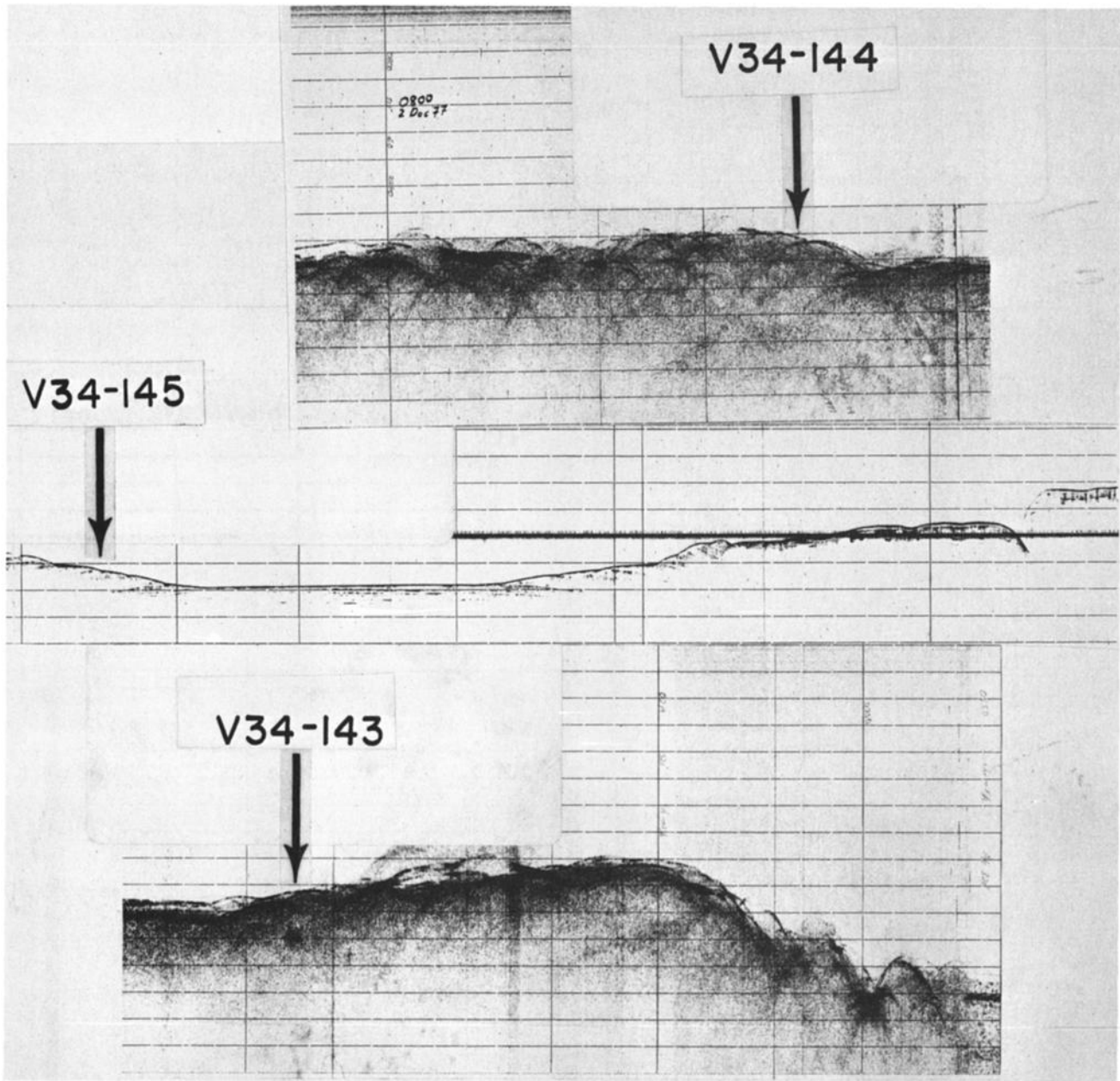
Fig. 3. The 3.5-kHz records of the sedimentary environment near cores 143, 144, and 145. One vertical division of the paper equals 20 fathoms (32.5 m).

samples with rock fragments are 3 to 10 x 10^{-5}cm/s, about 2 orders of magnitude higher than the permeability value measured for pelagic material (8 x 10^{-7} cm/s). This raises the possibility that the sediment-basement interface could serve as a conduit for water movement in areas where the bottom pelagic sediment is too impermeable for direct upward movement. Such a system would 'vent' where the sediment cover is thinnest.

Core 144 is from near the top of a small rise with thinner sediment cover than the surrounding area (Figure 3). The temperature profile from this core is nonlinear, implying a water movement rate of about 6 x 10^{-7} cm/s $\pm15\%$ [Bredehoeft and Papadopulos, 1965]. We feel that using such a steady state model is justified because the sedimentation rate in the area is at most 4 m/m.y. and

the sediment thickness is less than 250 m. Any transient flow or moving boundary effects caused by sedimentation are thus spread over extremely long time periods. In contrast, the water movement rate we infer is about a centimeter per year, more than 10^5 times greater than the sedimentation rate.

Our permeability values as given are actually hydraulic conductivites measured on a falling head apparatus. These hydraulic conductivities are corrected to the viscosity and density of sea water at 2°C and 500 atm. We will continue to refer to our hydraulic conductivity as permeability.

The lowest permeability measured on core V34-144 was 2 x 10^{-7} cm/s (Figure 4). From Darcy's law we know that the velocity of water movement (cm/s) equals the permeability (cm/s) times the gradient (dimensionless). This implies that a
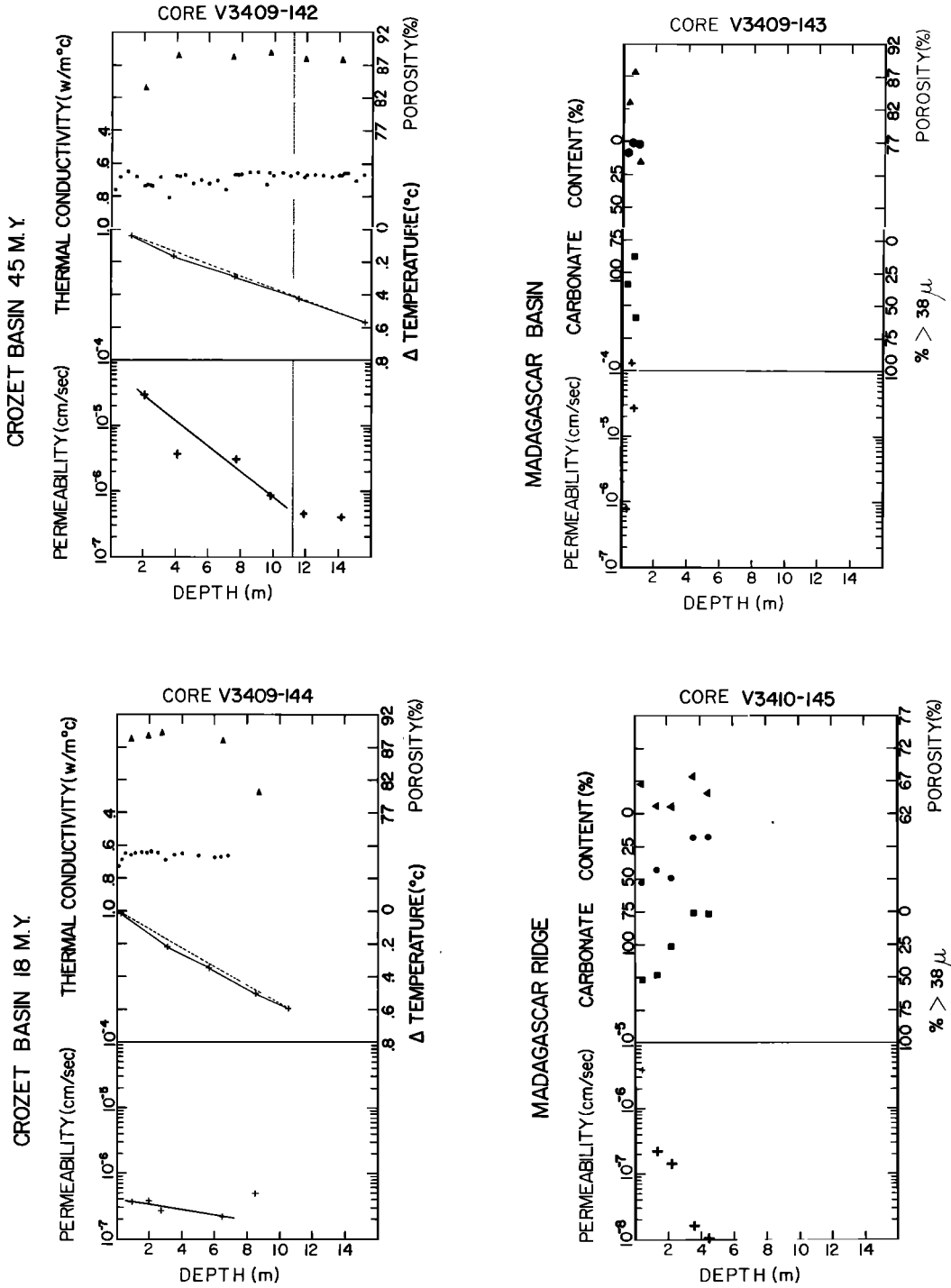
Fig. 4. Porosity (triangles), thermal conductivity (small dots), or carbonate content (large dots), temperature (crosses) variation with depth in cores 142, 143, 144, and 145. The dotted lines represent the beginning of flow-in in the core. The dashed line with the temperature measurements represents a perfectly linear temperature gradient. One centimeter per second equals approximately 1 kdarcy. Cores 142, 143, and 144 are predominantly brown clays. Core 144 has a bottommost sample which is 42% carbonate. On core 142 the top two samples have carbonate contents of 40% and 12% respectively. All other samples are 1% carbonate. All other samples in core 142 have less than 1% carbonate content.
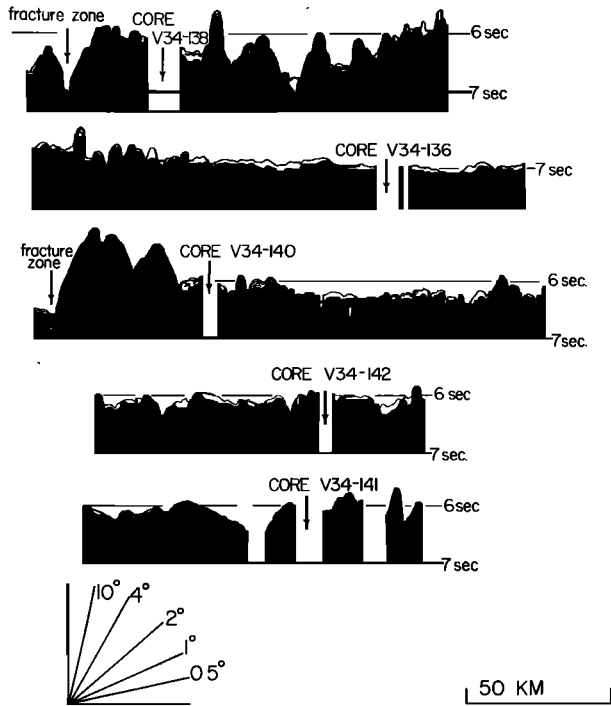
Fig. 5. Profiler records of the sedimentary environment in the vicinity of cores 136, 138, 140, 141, and 142. One second of two-way travel time equals 400 fathoms. The slopes and distances are for an average speed of 9 knots/h.

gradient of 3 exists at the point of lowest permeability in the sediment. A gradient near zero would imply normal hydrostatic conditions; values greater than zero require excess pore pressures in the sediment.

The next heat flow survey area is on 25 m.y. old crust in the Crozet Basin (Figure 5). Of 17 temperature measurements, 10 had nonlinear gradients. The mean of all measurements when corrected for convection approaches, but is still below, the theoretical value for seafloor of this age. The sediment cover in this area is thicker than in survey 1 (about 40 m), but some outcrops of basement rock still occur. These act as chimneys through which seawater transfers heat directly from basement to the ocean. The core for this area V34-141 has the greatest degree of nonlinearity observed in this study (Figure 6). The water velocity predicted by the nonlinearity of the temperature gradient is about 10^{-6} cm/s. Note that the temperature profile in this case as in all others could not be caused by the observed change in thermal conductivity. The lowest permeability measured is about 10^{-7} cm/s (Figure 6). This implies that a gradient of 10 exists at the point of lowest permeability. This is an absurd value, implying that the excess pore pressure is 10 times the effective weight of the overburden. This discrepancy will be discussed in detail below.

Two more heat flow surveys were made, one on 45 m.y. old crust in the Crozet Basin and the other on 55 m.y. old crust in the Madagascar Basin. Both of these surveys yielded average heat flow measurements slightly greater than that predicted by the theory when corrected for the effects of convection. This slightly higher mean is

of no great concern because of the limited number of measurements in the survey areas and because the heat flow values in the older portions of the Indian Ocean in general, seem to lie slightly above the theoretical values [Anderson et al., 1977].

Cores 136 and 140 in the Madagascar Basin show a semilog rate of decrease of permeability with depth (Figure 6). This semilog pattern appears in all brown clay cores which have relatively uniform carbonate and coarse fraction contents (cores 144, 140, 136, and 141; Figures 4 and 6). This pattern is probably a direct result of two processes associated with compaction, deflocculation, and water loss. The permeability of a flocculated sample was found to be 3 to 60 times higher than that of a sample of identical porosity but with a dispersed structure [Lambe and Whitman, 1979, p. 291]. Water loss would put the sediment in a less flocculated state and so lower its permeability. Shearing of the sediment caused by coring disturbance would also have a similar effect.

The change in permeability also correlates with a change in porosity, since water loss in a sediment should cause a decrease in porosity. This effect is difficult to observe directly without many measurements, since the local variability of porosity is so high (about $\pm2\%$). The brown clay core which has the steepest permeability fall off with depth (core 141) also shows the most clear-cut drop of porosity with depth. Bryant et al. [1970] found strong correlation between the log of permeability and porosity with the rate of change of permeability with porosity greatest for the most coarse-grained materials. The semilog fall of permeability with depth that we observe in the brown clay cores of uniform composition 136, 140, and 141 (Figures 4 and 6) is probably best attributed to a linear change in the average porosity with depth. This change is visible in the thermal conductivity measurements for cores 142, 141, and 144, since thermal conductivity is a direct function of water content and thus of porosity in cores with a uniform carbonate content.

Deviations from this pattern of semilog permeability decay with depth appear in the top of core 142 and the base of core 144, where the sediment has a carbonate content above 1% and a higher coarse fraction, thus resulting in a higher permeability and lower porosity.

Again the heat flow results for core 141, 142, and 144 provide us with estimates of the velocity of water movement through the sediment. The nonlinearity of core 142 is small enough to be within experimental error; nevertheless, the water velocity we derive from the nonlinearity is about 10^{-7} cm/s. This is enough to produce a gradient of about one third at the point of lowest permeability in the core.

Discrepancy Between Velocities Determined from
Heat Flow, Permeability, and Darcy's Law

Permeability measurements imply higher excess pore pressures than could be supported by the sediments, assuming the velocities of transport derived from heat flow are correct. At least three major possible causes for this discrepancy exist: (1) undisturbed clay-rich sediments have a higher cohesion intercept (cohesive strength at zero effective stress) than that measured in lab-
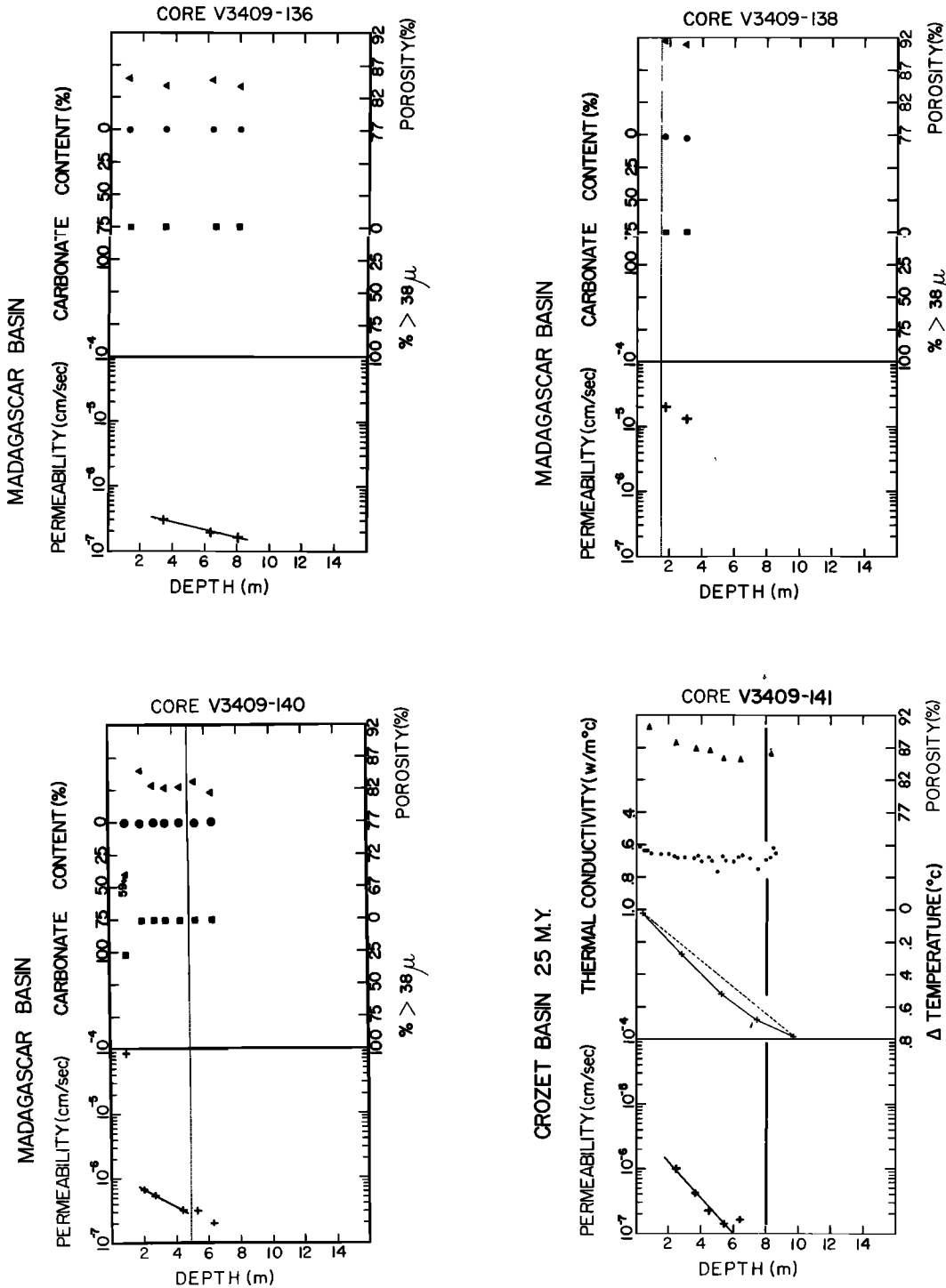
Fig. 6. Porosity (triangles), thermal conductivity (small dots), or carbonate content (large dots), temperature differences (crosses), or percent greater than 38 microns (squares), and permeability (crosses) variation with depth in cores 138, 140, 141, and 136. The dotted line represents the approximate beginning of flow-in in the core. The dashed line represents a perfectly linear temperature gradient. One centimeter per second equals approximately 1 kdarcy. The cores are predominantly brown clay, with less than 2% carbonate content. The topmost sample in core 140 is a micromanganese nodule sand.

oratory experiments and so can support substantial excess pore pressures for some period of time, (2) the water movements causing the nonlinear temperature gradients are predominantly horizontal rather than vertical, and (3) the laboratory measurements of permeability are lower than the in situ values.

The cohesion intercept (τ_c) for clay-rich terrestrial soils varies from 4.8 - 24 kN/m^2(4.8 - 2.4 x 10^5 dynes/cm^2) [Lambe and Whitman, 1979, p. 316]. The greatest difference between the calculated overburden pressure and the excess pore pressure (gradient of 10 in core 141) is 1.2 x 10^6 dynes/cm^2, much higher than the maximum measured values of the cohesion intercept in terrestrial clays. If we assume that the clay in core 141 has the maximum cohesion intercept, then the ratio of the excess pore pressure to overburden pressure plus cohesion intercept is still a factor of 3. The cohesion intercept of in situ marine clays would have to be 3 times higher than laboratory values to explain this inconsistency. This is unlikely to be a viable alternative because water content and cohesion intercept are inversely related. The water contents of the terrestrial clays with the highest cohesion intercept are less than 25%. In contrast, the marine clays in the southwest Indian Ocean have water contents from 80 to 91%. It thus appears likely that the cohesion intercept of the clays in the survey areas is much less than the maximum values obtained in laboratory experiments upon terrestrial samples.

Horizontal water movement along the sedimentary layers can generate nonlinear temperature profiles, provided that a source of anomalously hot or cold water is nearby. A vertical crack in the sediment or a steep abyssal hill can act as a source for this water. Both cores V31-141 and V34-177 are located in regions of rough topography which are possible locations of sources of this kind. Horizontal water movement can dominate vertical water movement because a horizontally layered material has a vertical permeability controlled by the most impermeable layer but a horizontal permeability determined by the most permeable layer [Lambe and Whitman, 1979, p. 275].

Additionally, the presence of small fluctuations of porosity about the normal increase with depth can cause large differences in the permeabilities of nearby layers. This is because a change in porosity of a few percent can cause an order of magnitude change in the permeability (Figure 6). Cores 136, 138, 141, and 140 are the best examples of this because they lack carbonate-containing surface layers. The 1-2% fluctuations in porosity will not substantially affect the vertical permeability but may cause the average horizontal permeability to be much higher than the vertical permeability. The platelike shape of the clay mineral particles, which tend to align themselves with their long axis horizontally as compaction proceeds, would further increase the difference between the average horizontal and vertical permeabilities. A ratio of horizontal to vertical permeability of 2 to 10 times is common in normally consolidated terrestrial clay [Lambe and Whitman, 1979, p. 275].

We have developed a simple model of horizontal water movement with which we can study the shape of the temperature profile and the rate at which nonlinearities in the temperature profile decay as

the distance from the anomalous water source increases (Appendix A). In our model, water enters the sediment from a vertical surface at a constant temperature and then flows horizontally (Figure 9). The water velocity is controlled by the permeability of the sediment, which may be constant or decrease with depth. When the sediment has a constant permeability, the temperature profiles are bow shaped. The bow is concave upward when the temperature of the anomalous water at its source is near the bottom water temperature. The bow is concave downward when the temperature of the source water is relatively warm. Horizontally moving cold water produces a temperature profile similar in shape to one caused by downward vertical flow, while horizontally moving water produces a profile similar to that caused by upward vertical flow. When sediment permeability decreases with depth, the shape of the temperature - profile becomes increasingly distorted (Figure 10).

The degree of nonlinearity depends upon the velocity of the horizontally moving water, the size of the source, and the distance from it. For an average horizontal permeability of 5 x 10^{-6} cm/s and a 10-m-long source some nonlinearity should be visible up to about 6 m away from the source.

The vertical permeability of core V34-144 is nearly constant with depth and has a value of 5 x 10^{-7} cm/s. Even if we assume the horizontal permeability is 10 times larger than this value, sources that affect the temperature profile must be within 6 m of the core. The nearest outcrop to this core is 80 m distant, but the presence or absence of cracks was not determined. Core V34-141 has a surface vertical permeability which rapidly decreases with depth. Anomalous water sources that affect this core must be no more than about 16 m distant, while no outcrops are observed within 200 m of the core. Therefore we can discount basement outcrops as sources for nonlinear temperature profiles for both of these cores. Cracks in the sediment are unlikely sources for the nonlinear temperature profiles in cores 141, 142, and 144. All of these cores have convex upward temperature profiles which would require horizontal movement of warm water emitted from a crack. The lower part of the crack would need to be kept open by the water flow, yet the crack could not extend to the surface or horizontal flow would not occur. The cracks would need to stop within centimeters of the surface to produce the temperature profiles that we observe. This seems unnecessarily fortuitous. Additionally, worm burrows are often preserved at several meters depth within cores, so that fractures if they exist should have been observed. We did not observe cracks in the Indian Ocean cores nor do we know of any fractures at depth in other deep sea cores. We thus feel that warm water cracks are unlikely sources of the nonlinear temperature gradients we observed. Thus, although we cannot rule out horizontal water movement in every case, it is not the cause of the nonlinear gradients in cores 144 and 141.

Another possibility is that the permeabilities we measured in the lab are actually lower than the in situ values of the permeability. Our device measured the saturated sample at about 1 bar, but the in situ pressure is about 500 bars. Although our measurements as a group agree with those of

TABLE 1. Summary of Core Data

| Age of Oceanic Crust (my) | Core Number | Slope of Permeability - Depth Profile (Decades/m) | Depth of Core Barrel Penetration / Good Core (cm) | Amount of Flow-in in Core (%) | Grain Size Distribution | | Proportion of Nonlinear Temperature Profiles in Area (%) | Approximate Surface Sedimentation Rate (m/my) |
					% > 38µ ± 0.1%	% > 4µ ±10%		
55	136	0.05	1210/1006	0	0.18	75	46	4
55	138	--	235/158	59	--	--	46	4
55	140	0.13	725/563	14	1.02	62	46	4
25	141	0.28	1020/800	23	0.39	68	59	2
45	142	--	1615/1016	42	0.77	33	33	3
18	143	--	106/106	0	35.00	45	65	1
18	144	0.04	1110/660 → 895 ?	0?<27	0.30	65	65	1
>55	145	--	?/514	0	49/26/1	89	--	>1.5*
>55	148	0.10	1180/1006	5.2	6.00	77	--	>6.6*
>80	151	0.33	450/370	0	20.00	55	--	>2.0*
>80	155	0.48	?/230	0	37.00	41	--	>2.9*
>80	156	0.13	605/516	0	21.00	53	--	>1.3*

* Determined from dating of the base of fossiliferous plateau and ridge cores.

Bryant et al. [1970] for clays, none of the existing measurements have been done at pressures higher than about 20 bars. Measurements do exist for the electrical resistivity of montmorillonitic clay-water solutions for pressures between zero and 2500 bars [Lang, 1967]. The resistivity of the montmorillonite-water solution increases irregularly for pressures between zero and 500 bars, while above 500 bars the resistivity changes smoothly with pressure. Lang [1967] attributes this behavior to the loss of adsorbed water on the clay mineral surfaces, which becomes complete at 500 bars. Adsorbed water on clay mineral surfaces would cause measurements at low pressures to underestimate the in situ permeability. Since the clay fraction of sediments from the southwest Indian Ocean tends to have a high montmorillonite content (50-70%) [Kolla, 1976], such a mechanism could be important in determining the in situ permeability of the sediments. There is thus a great need for the development of in situ permeability measurement capabilities.

Aside from the problem of duplicating in situ conditions, there is also the problem of sediment disturbance. As cited previously, remolding of sediments can lower the permeability by a factor of 3 to 60 [Lambe and Whitman, 1979, p. 291]. Even a small amount of disturbance could lower the permeability sufficiently to cause a discrepancy between the measured permeabilities and the calculated water velocities. In addition to this, the higher the excess pore pressures, the lower the strength of the sediment will be. This is because the strength of a sediment is proportional to the effective stress (the overburden pressure minus the pore pressure) rather than the total stress (the overburden pressure)[Lambe and Whitman, 1979, p. 241]. The sediments with the highest excess pore pressures will thus be the most likely to be remolded, with consequent lowering of the measured permeability.

What evidence exists for sediment remolding

during coring? Remolding caused by high excess pore pressures may result in the presence of large amounts of material classified as flow-in. Both cores 141 and 142 have large amounts of flow-in and nonlinear temperature gradients. The depths of penetration in both cores are constrained to within 10 cm by the heat flow. Flow-in is core material that looks disturbed and appears turbulently mixed with most layering vertical rather than horizontal. The traditional view of flow-in is that it is material sucked in by the core pipe as the pipe is removed from the bottom. In such a case the core should be longer than the total depth of penetration. In the case of core 142 the core is 1700 cm long with 1615 cm of penetration. Of the 1700 cm of core, 700 cm are classed as flow-in. In order for all of this material to be the result of the pullout the core would need to have triggered 6 m too late and then to have drawn in 7 m of material on the pullout. Core 141 has 1021 cm of penetration and is 1078 cm long; 278 cm of this core are classified as flow-in. In order for all the material in the pipe classed as flow-in to be displaced material, a 220-cm late trigger and 278 cm of material pulled in upon with withdrawal of the core are needed.

An alternative interpretation is that most of the material classified as flow-in is actually drawn in during the penetration of the core pipe. If water velocities indicated by the heat flow measurements are correct, excess pore pressures which approach the overburden pressure are predicted at shallow depths in the sediment. Such a highly overpressured zone could easily be fluidized by the impact of coring. This liquified material could then be turbulently sucked into the core pipe during penetration. Material from such an overpressured zone would show a virtually constant permeability with increasing depth, precisely what we see in material classified as flow-in in cores 141 and 142.

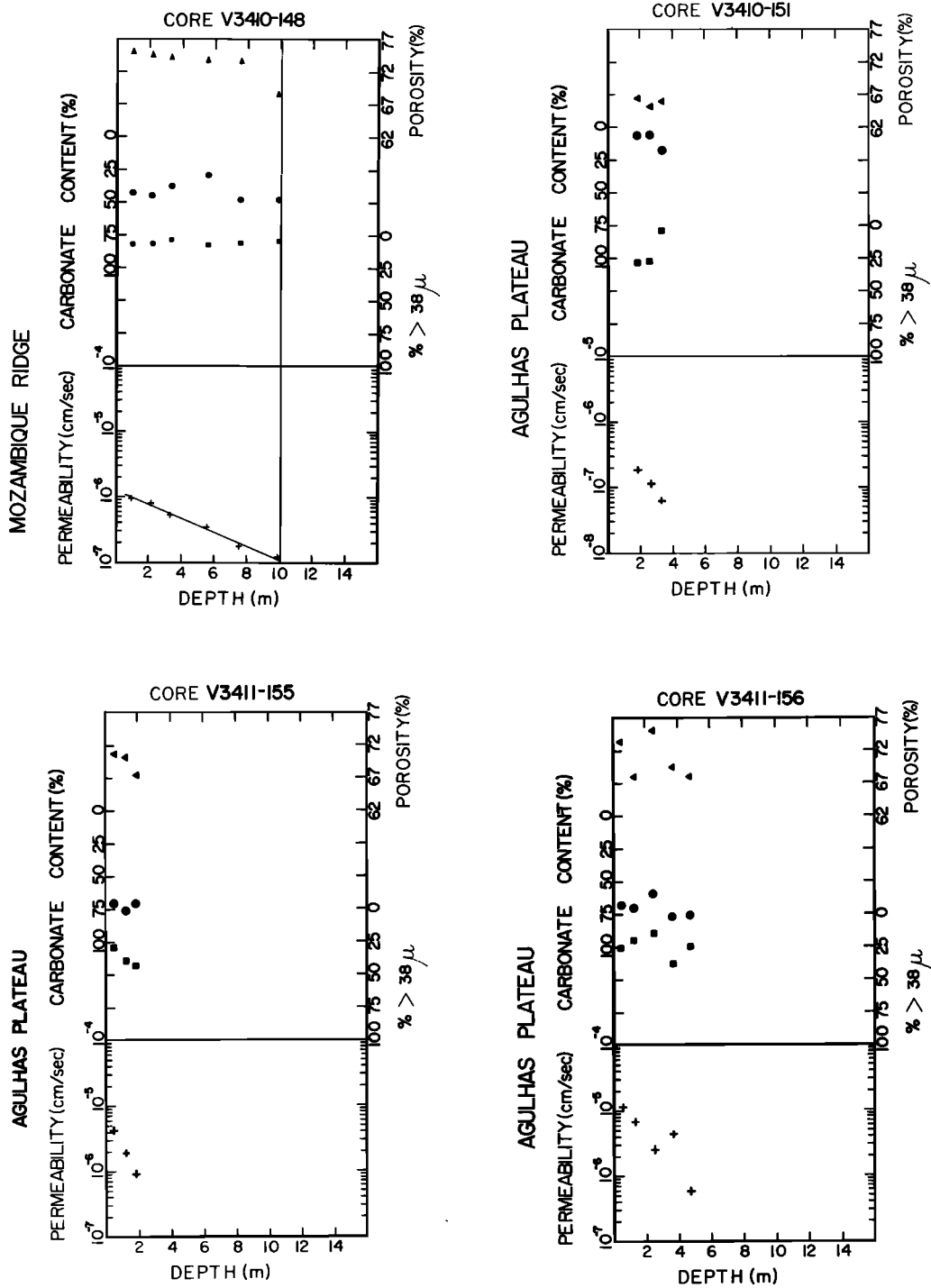Flow-in is quite common in the cores from areas

Fig. 7. Porosity (triangles), carbonate content (circles), percent greater than 38 microns (squares), and permeability (crosses) distribution with depth for cores 148, 151, 155, and 156. Dotted line is approximate beginning of flow-in in core 148. One centimeter per second equals approximately 1 kdarcy.

with nonlinear gradients, while only one of the calcareous cores has flow-in (see Table 1). Although flow-in could be partially related to a high clay content, the calcareous cores discussed below have analogous clay percentages, so that the difference in amount of flow-in is indeed significant. Among the red clay cores where flow-in is absent, core 136 is from the deepest and oldest seafloor (Figure 5), while core 143 has high permeability and rock fragments at its base. We are ignorant of flow-in in core 144 because the last pipe was lost in transit, but it is definitely less than 27% of the core.

The evidence from flow-in thus appears to support the idea that excess pore pressures do indeed exist in the core locations where nonlinear temperature gradients were measured. This would tend to support the idea that water is moving through the sediment, as the heat flow measurements suggest. The laboratory measurements of permeability would have to be low by only an order of magnitude in order to resolve the discrepancy between velocities calculated from heat flow versus permeability, assuming that significant excess pore pressures exist. Such a variation in permeability from in situ to laboratory conditions is well within the range of changes caused by remolding.

What other evidence exists for high excess pore pressures in the sediment of the Madagascar and Crozet basins? Abyssal hills and hillsides which are virtually bare of sediment are visible in the areas of nonlinear gradients, particularly in the 18 and 25 m.y. old survey areas (Figures 5 and 2). The amount of sediment cover seems partially but not totally related to the steepness of the topography. Although current activity could be the cause of the uneven sediment cover, another possibility is that areas of upwelling water cause periodic sediment slides or slumps on topographic highs. Because the compaction of sediment under its own weight produces a decrease in permeability with depth, a constant flux of water through the sediment will produce an increase in excess pore pressure with depth (Appendix B). Thus when the excess pore pressure in the sediment exceeds the combined force of the overburden pressure and the cohesive strength of the sediment, the cover becomes unstable and slides or slumps. The critical thickness would depend upon the permeability and the rate of water movement through the sediment. Such slumps or slides might produce graded bedding but not of the classic form, since brown clays are all fine grained. Instead of graded bedding discernable to the naked eye the grading of the beds would only appear as the result of careful grain size work. Such grading could produce local variations in porosity, permeability, and thermal conductivity. We found probable slump masses on the 3.5 kHz records for cores V34-143 and V34-144 (Figure 3). We were unable to use fossils in this area to detect slumping because the cores have no fossils or a few severely dissolved fossils.

The average apparent sedimentation rate of the survey areas increases with age (Table 1), an observation possibly attributable to overpressures. The major sources of sediment in the three younger survey areas are predominantly pelagic and weathered basement material. All cores are from below the Carbonate Condensation Depth (CCD). In this case, one would expect the youngest areas to have the highest rather than the lowest average apparent sedimentation rate. Compaction effects and increased seismic velocity would tend to accentuate the expected higher sedimentation rate in younger areas. The effects of water movement provide a mechanism for lowering the sedimentation rate in the youngest areas, since sediment slides or slumps of fine-grained material would facilitate resuspension and removal by currents. In areas of rapid water movement the fluxes we calculate are high enough to prevent Stokes law settling of very fine material (less than 1/2 micron).

Calcareous Sands and Muds

The cores containing calcareous sands and muds have no heat flow data, but large amounts of water movement are considered unlikely due to the locations of the cores (Figure 1) [Anderson et al., 1977]. The hills and ridges in these areas are continuously draped with sediment, even upon fairly steep slopes (Figures 2 and 3).

The 3.5-kHz record for core 145 shows a layered sediment with no probable slump masses, even on the steep slope at the far right (Figure 3).
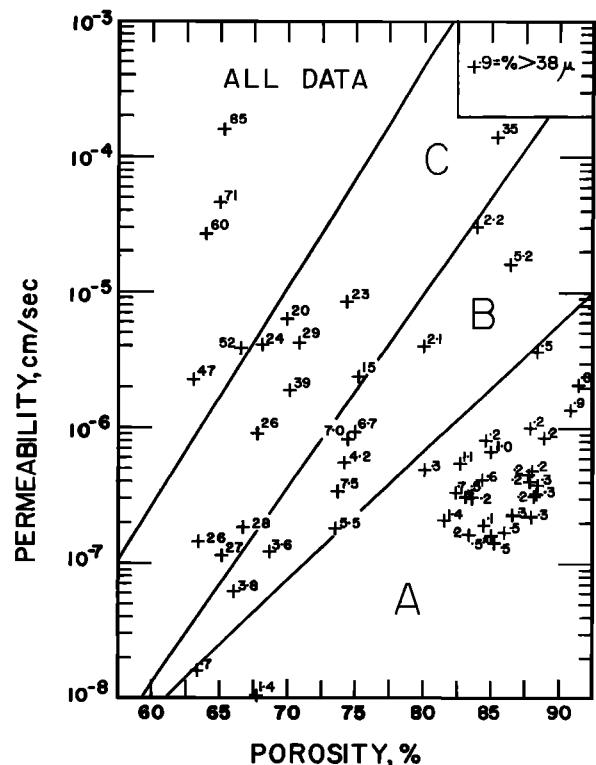

Fig. 8. Permeability plotted versus porosity for all samples. The numbers next to the sample data points (crosses) represent the percent of the sample larger than 38 microns. The three groupings (A, B, and C) represent samples with the following range of percent coarse fraction: A, less than 1.5; B, 1.5 → 15; C, 15 → 50. Notice that the rate of change of permeability for the same change in porosity is higher in groups B and C than it is in group A. One centimeter per second equals approximately 1 kdarcy.

TABLE 2. The Constants A_i, B_i, C_i (the Top, Middle and Bottom
Number of Each Group) for several values of i and p

p = 0	p = 1	p = 2	p = 3
	n = 1		
-1.414	-0.908	-0.670	-0.531
+2.828	+2.374	+2.165	+2.044
+3.141	+2.903	+2.781	+2.707
	n = 2		
-1.000	-0.561	-0.384	-0.289
0.000	-0.458	-0.645	-0.744
+6.283	+6.033	+5.906	+5.830
	n = 3		
-0.816	-0.425	-0.279	-0.206
+1.632	+1.251	+1.112	+1.042
+9.425	+9.170	+9.042	+8.965
	n = 4		
-0.707	-0.349	-0.224	-0.162
0.000	-0.363	-0.490	+0.552
+12.566	+12.305	+12.174	+12.095

Erosion effects are definitely present, but there is no evidence of the acoustically vague, unlayered sediment which occurs near cores V34-143 and 144. However, an extrapolation of the surface trends would produce quite low permeability at depths of several tens of meters. These permeabilities are low enough so that excess pore pressures could develop in the presence of high water fluxes. Thus the absence of bare slopes of basement rock might be evidence against high excess pore pressures and water fluxes in this region.

With the exception of core 145, all of the calcareous sands and muds have a relatively small range of grain sizes. Cores 148, 151, 155, and 156 all show a semilog rate of decrease of permeability with depth. This is probably again attributable to a linear fall off of the average porosity with depth (see Figure 7). Because of larger local deviations in the porosity this effect is not as obvious, but it is present. The importance of this semilog fall-off of the permeability with depth is that it predicts quite low permeability at shallow depths in the sediment, provided that compaction is not affected by excess pore pressures. Although the compaction at the surface is no doubt more rapid than that which occurs at depth, very low permeabilities are still likely at shallow depths.

The other importance of the semilog pattern is that the slope of the permeability-depth profile is correlatable with the average percent coarse fraction (Table 1). This is not too surprising, since the higher percent coarse fraction material has a greater average permeability (see Figure 8). Thus percent coarse fraction, porosity, and permeability are all intimately related. A marine material with a higher percent coarse fraction will compact more quickly for three reasons, (1) it has a higher permeability, (2) the fossils which are in the coarse fraction crush easily, and (3) fossils, heavy minerals, and rock fragments do not have adsorbed water on their surfaces, as clay minerals do.

The contrast between the calcareous material and the brown clays points out the importance of

grain size distribution in determining the slope of permeability-depth profiles. These profiles have the potential to be used as indicators of the effects of excess pore pressure and water movement upon the compaction of the sediment, but the effect of grain size distribution must first be removed.

Summary

We have presented a number of lines of evidence that excess pore pressures do exist in the areas of red clay sediment in the southwest Indian Ocean: (1) the presence of turbulently mixed material at the bases of cores with nonlinear temperature gradients and low permeability, (2) the lack of sediment cover on hillsides and hilltops in the red clay areas, whereas similar features which are present on the aseismic ridges and plateaus are thickly sedimented, (3) the increasing average apparent sedimentation rate with age in the Crozet and Madagascar basins, and (4) the presence of nonlinear temperature gradients and sediments of low permeability in the Madagascar and Crozet basins.

There are still a number of contradictions; the most important of which is that the laboratory measurements of permeability appear to be too low to allow water movement. Because the major disturbing effects of coring would all act to cause the laboratory measurements of permeability to be lower than their in situ values, we believe that an in situ measurement program of permeability and excess pore pressure is necessary. Measurements of these two variables would show definitively the presence or absence of the water fluxes indicated by the heat flow and other data.

We are presently attempting to measure both in situ excess pore pressures and permeability in locations which are known to have nonlinear temperature gradients. We are also working with geochemists to do pore water studies on cores with heat flow and excess pore pressure measurements. These measurements, which are all independent, should help us to resolve our present problems.

Appendix A: Horizontal Water Movement and Temperature Profiles

The Model. We will consider a sediment of uniform thermal properties that in the absence of horizontal water movement has a linear temperature profile. At a reference depth z=0 in the sediment the temperature is T_B. At the top of the sediment, z=L, the temperature is zero. We will calculate the effect of water which enters a vertical crack at temperature T_C located at a horizontal range x=0. The crack extends vertically from z=0 to z=L. The water velocity varies with depth, since it is proportional to the sediment's permeability. We will assume that the variation can be adequately represented by a known function of depth $V_H(z)$= $V(z/L)^p$, where V is the horizontal pore-fluid velocity at the top of the sediment and p is an integer describing how fast the velocity decreases with depth (that is, increases with z). This geometry is shown in Figure 9.

We will also assume that the temperature distribution does not vary with time and that heat is transferred vertically only by conduction and horizontally only by water movement. Under these circumstances the equation of heat flow is:

$$n\rho c\ V_H(z)\ \frac{\partial T}{\partial x} = k\ \frac{\partial^2 T}{\partial x^2} \qquad (A1)$$

where ρ and c are the density and heat capacity of sea water, respectively, and n and k are the porosity and thermal conductivity of wet sediment, respectively.

The Solution. The temperature distribution is then given by [see Hildebrand, 1962, p. 158]:

$$T(x,z) = T_B \times (1-z/L)\ +$$

$$\sum_{i=1}^{\infty} [A_i T_B + B_i T_C]\ (z/L)^{\frac{1}{2}}\ J_{\frac{1}{p+2}} [C_i(z/L)^{\frac{p+2}{2}}]\ \exp\ (D)$$

$$\text{where } D = -\frac{1}{4}\ C_i^2\ (p+2)\ \frac{k}{n\rho cV}\ \frac{x}{L^2} \qquad (A2)$$

Here J is the fractional order Bessel function of the first kind, and A_i, B_i, and C_i are constants (see Table 2).
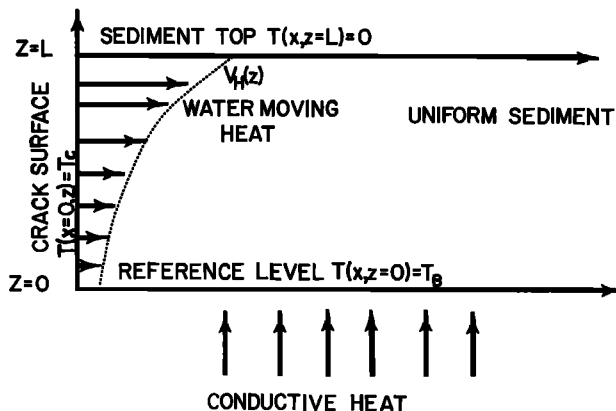

Fig. 9. Schematic of problem showing geometry and boundary conditions.

TABLE 3. The Critical Crack Temperature T_C(critical) and the characteristic distance x_C as a function of p (i.e. the velocity - depth profile)

	p=0	p=1	p=2	p=3
T_C(critical, % of T_b	0.500	0.382	0.309	0.260
x_C, m ($v = 5 \times 10^{-6}$ cm/s)	2.66	1.39	0.84	0.57
x_C, m ($v = 5 \times 10^{-5}$ cm/s)	26.0	13.9	8.4	5.7

Calculations are for the data given in Figure 10 and two different water velocities.

The first term in the solution contains the linear gradient. At very large ranges, corresponding to distances far from the crack where the water temperature has completely equilibrated, the exponentials cause the terms in the summation to be nearly zero. At these large ranges the temperature profile is nearly linear. Since the constants C_i rapidly increase with i, only the first term of the summation is important at intermediate ranges. Then the temperature profile consists of a linear gradient modified by a bow shaped Bessel function. The size of the bow depends upon the size of the exponential. The characteristic decay distance (see Table 3) is given by:

$$x_C = -\frac{4}{C_1^2\ (p+2)^2}\ \frac{n\rho cV}{k}\ L^2 \qquad (A3)$$

For reasonable choices of the constants the characteristic distance is between 1 and 20 m. Depending upon the crack temperature, the bow shaped Bessel function is either added to or subtracted from the linear gradient. For crack temperatures near zero (the bottom water temperature) the temperature is less than that of a linear gradient
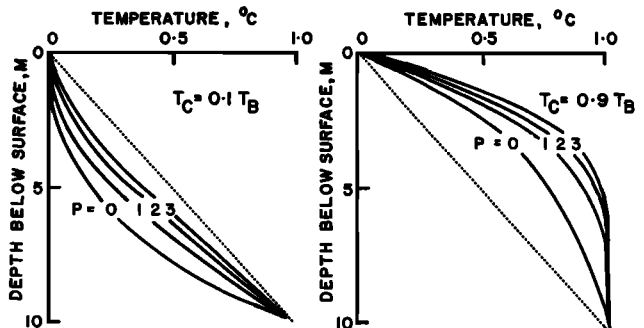

Fig. 10. Plot of temperature-depth profile for two different choices of T_C and for several different velocity-depth functions (p = 0, 1, 2, 3). The average velocity in the interval from 0 to L is the same in all cases; $V_H = 5 \times 10^{-5}$ cm/s. The dotted line is the linear gradient. Constants used (oceanic sediment): = 1.04 g/cm^3; k = 1.6 x 10^{-3}cal/s cm °K; c = 0.9 cal/g °K; n = 0.9; L = 10 m; x = 10 m; T_B = 1.0°C.

TABLE 4. Overburden Pressure and Excess Pore
Pressure Calculated for Core V34-141

Depth, m	P_o, dynes/cm^2	P_e, dynes/cm^2
1	1.5×10^4	3.9×10^3
2	3.3×10^4	3.3×10^4
3	5.3×10^4	1.3×10^5
4	7.5×10^4	3.4×10^5
5	9.8×10^4	7.1×10^5
6	1.2×10^5	1.3×10^6

(bow subtracted). For crack temperatures near T_B it is greater (bow added). The temperature at which the bow neither adds or subtracts, the critical temperature T_c(critical) is (see Table 3 and Figure 10):

$$T_c(\text{critical}) = - A_1 T_B / B_1 \quad (A4)$$

In the case of a constant horizontal water velocity (P=0), the critical crack temperature equals (as expected) the average of the temperature at the top and bottom of the sediment.

Appendix B: Overburden Pressure and Excess Pore
Pressure Calculated for Core 141

Core 141 had the highest upward water flux of those cores observed to have nonlinear temperature gradients. The following relations [from Lambe and Whitman 1979] were used to calculate the excess pore pressure, P_e and the overburden pressure P_o:

$$P(z) = \int_0^z \frac{\rho_w \, g \, v(z) \, n(z)}{k(z)} \, dz \quad (B1)$$

$$P(z) = \int_0^z (\rho_s - \rho_w) \, g \, [1 - n(z)] \, dz \quad (B2)$$

Here ρ_w and ρ_s are the densities of water and sediment particles, g is the gravitational acceleration, v(z) is the water velocity in the sediment, and n(z) is the porosity as a function of depth. The product n(z)v(z) is a constant, here 1×10^{-6} cm/s.

Calculations based on these relations, shown in Table 4, predict that the excess pore pressure exceeds the overburden pressure at only 2 m depth. If this were so, the permeability would cease to decrease or decrease very slowly below 2 m. In actuality, the permeability continues to decrease rapidly until 6 m depth, where it attains a value (measured in cm/s) which is less than 1/10 the predicted water velocity. All samples below this depth are classed as flow in.

As discussed earlier, we believe that this flow-in is largely material which had an initial in situ excess pore pressure. The impact of coring caused fluidization of this zone, which then flowed in during penetration of the core pipe.

The amount of excess pore pressure generated by the coring process itself would determine the in situ excess pore pressure necessary for fluidization.

REFERENCES

Anderson, R. N., M. G. Langseth, and J. G. Sclater, The mechanisms of heat transfer through the floor of the Indian Ocean, J. Geophys. Res., 82, 3391-3409, 1977.
Bredehoeft, J. D., and I. S. Papadopulos, Rates of vertical groundwater movement estimated from the earth's thermal profile, Water Res., 1, 325-328, 1965.
Bryant, W. R., W. Hottman, and P. T. Trabant, Permeability of unconsolidated and consolidated marine sediments, Gulf of Mexico, Mar. Geotech., 1, 1-13, 1970.
Embley, R. W., and R. D. Jacobi, Distribution and morphology of large submarine sediment slides and slumps on Atlantic continental margins, Mar. Geotech. 2, 205-227, 1977.
Hildebrand, F.B., Advanced Calculus for Applications, Prentice-Hall, Englewood Cliffs, N. J., 1962.
Keller, G. H., and R. H. Bennett, Sediment mass physical properties-Panama Basin and northeastern equatorial Pacific, Initial Rep. Deep Sea Drill. Proj., 16, 499-512, 1973.
Kolla, V., L. Henderson, and P. Biscay, Clay mineralogy and sedimentation in the western Indian Ocean, Deep Sea Res., 23, 949-961, 1976.
Lambe, W. T., and R. V. Whitman, Soil Mechanics, John Wiley, New York, 1979.
Lang, W. J., The influence of pressure on the electrical resistivity of clay-water systems, Conf. Clays Clay Minerals, 15th, 455-468, 1967.
Parsons, B., and J. G. Sclater, An analysis of variation of ocean floor heat flow and bathymetry with age, J. Geophys. Res., 82, 803-827, 1977.
Saito, T., L. H. Burckle, and J. D. Hays, Implications of some pre-Quaternary sediment cores and dredging studies in paleooceanography, S.E.P.M. Short Course, 20, 6-36, 1974.
Schlich, R., Structure et âge de l'Océan Indien Occidental, Mem. Soc. Geol. Fr., 6, 1975.
Simpson, E. S. W., et al., Leg 25 DSDP western Indian Ocean, Geotimes, 21-24, 1972.
Trabant, P. K., Synthesis of physical properties

data from DSDP leg 41, Initial Rep. Deep Sea
Drill. Proj., 41, 1199-1213, 1977.
Trabant, P. K., W. R. Bryant, and A. H. Bouma,
Consolidation characteristics of sediments from
leg 31 of the Deep Sea Drilling Project, Initial
Rep.Deep Sea Drill. Proj., 31, 425-432, 1975.
Tucholke, B. E., and G. B. Carpenter, Sediment

distribution and Cenozoic sedimentation patterns
on the Agulhas Plateau, Geol. Soc. Am. Bull.,
88, 1337-1346, 1977.